FULL RESEARCH ARTICLE

Optimizing energy modeling in PBF-LB/M metal additive manufacturing: a detailed analysis of resource and energy demand based on standard tensile test specimen

Joachim Brinkmann[1] · Jan C. Aurich[2] · Henrik te Heesen[1]

Abstract

Additive manufacturing is an essential tool in modern production processes. Competitive quality and the increasing importance of local manufacturing have allowed companies to maintain their production despite supply chains disrupted by the pandemic. However, the rising awareness of society towards environmental and climate protection, the increasing demand for resource-efficient products, and recent developments in energy costs are leading to a rethink in manufacturing processes. Additive manufacturing offers great potential for resource saving components. This study uses standard tensile test specimens to analyze AM processes regarding energy and material flows. The results show a high dependence of energy demand on process time and are transformed into a data-based energy model. Compared to previous energy models, the accuracy can be significantly improved using model data in combination with specific and system-oriented approaches. In addition to system-related saving potentials, design-related optimization potentials can be identified. Innovative and highly resource-saving components can be designed with a design methodology adapted to the extended degrees of freedom of AM. Further saving and recycling potentials can be identified along the material flows. A long-term goal is optimizing and predicting of resource demand in additive manufacturing with a view to the entire product lifecycle.

Keywords Additive manufacturing · PBF-LB/M · SLM · Resource efficiency · Energy model

1 Introduction and motivation

Additive manufacturing is an essential tool in innovative production processes. The extended degrees of freedom offer much potential in usage, construction, and product design [1]. Rising raw material and energy costs, constantly increasing environmental requirements, and the increasing demand for resource-saving products represent a paradigm shift in classic production processes [2].

✉ Joachim Brinkmann
  j.brinkmann@umwelt-campus.de
  http://www.umwelt-campus.de

  Henrik te Heesen
  h.teheesen@umwelt-campus.de

1 Trier University of Applied Science, Environmental Campus Birkenfeld, 55761 Birkenfeld, Germany

2 RPTU Kaiserslautern - Institute for Manufacturing Technology and Production Systems, 67663 Kaiserslautern, Germany

In addition to the purely energetic evaluation, developing energy models is a method to determine energy consumption and reduce it in the long term. The specific energy consumption model, also known as the SEC model, allows a quick estimation of energy consumption by multiplying the SEC with a unit like the mass of the workpiece, the manufacturing time, or the exposed area [3]. Here, high dependence on the used machine, the considered peripheral devices, and the geometry are noticeable.

Previous studies, such as those by Kellens et al. [4] and Baumers et al. [5], have laid the basis for understanding the energy demands of PBF-LB/M processes. Various energy models have subsequently been proposed, including those by Paul and Anand [6], Yi et al. [7], Lv et al. [3], and Hui et al. [8]. These models are often limited by their specificity to sub-processes or subsystems. This results in limitations in their applicability to other manufacturing machines or inaccuracies in energy consumption predictions. The simulation accuracy ACC is mostly in the range of 90% [3, 5, 9] with the limitation of small sample sizes. Moreover, nearly, all these models rely heavily on process time information,

making the accuracy of their simulations largely dependent on the quality of the underlying time model.

In the following study, two manufacturing machines of the PBF-LB/M process are analyzed and compared with other studies. The aim is to analyze the power and resource consumption to use these data to build an improved energy model with a high accuracy, which can be used as an additional parameter in the adapted design methodology. Furthermore, potential savings are derived from the load curves.

2 Definitions

2.1 Selective laser melting

Additive manufacturing encloses a wide range of possibilities for manufacturing different materials. This study aims to investigate the resource and energy consumption of metal additive manufacturing processes especially using the selective laser melting (SLM) process, also known as laser powder bed fusion or PBF-LB/M. Other methods such as FDM or SLS processes with an additional step of sintering are not considered.

Two production machines operating according to the PBF-LB/M principle are used to investigate the material and energy flows. A Renishaw AM400 and a newly developed MPrint from the company One Click Metal. Both operate with single-fiber lasers, the AM400 with a 400 W and the Mprint with a 200 W power laser. In addition to the building space parameters, the simple powder handling, and the compact dimensions of the MPrint are significant differences from the AM400 (Table 1).

The layer-by-layer structure, in which a controlled laser selectively welds metal powder in layers, produces complex three-dimensional structures. Kellens [4] divides the PBF-LB/M (SLM) process into four phases:

1. Prepare: initializing, preheating, inerting
2. Exposure: selective melting of the metal powder
3. Recoating: recoating with new powder
4. Post-processing: unpacking, separation from the construction platform, cleaning, and machine restoration.

The four steps are identical in both manufacturing machines, with only the inertization differing significantly. In the AM400, a vacuum is initially created in the build chamber by extracting the air. This is followed by flooding the chamber with Argon inert gas until the limit value of 1000 ppm is reached. The MPrint only inertizes based on the displacement principle with nitrogen up to an oxygen content of 6000 ppm. The unpacking occurs after the build process (phases 2 and 3).

2.2 Energy modeling

Based on Hui's [8] research, energy models can be divided into three categories: specific energy models (SEC), phase-based energy models and subsystem-based energy models.

Specific energy models use specific energy consumption multiplied by a characteristic value, such as mass or volume. Other attributes could be the exposure area or time, though only the area considers workpiece geometry, layer thickness, and orientation [6].

A sub-phase model, like that developed by Yi et al., divides the process into particular time and power model for each phase, such as preparation or cooling, allowing precise determination of energy requirements per step [7, 9].

Sub-system models differentiate between energy-related subsystems. Often, the equipment parts of the production machine are considered, such as the cooling unit, laser unit and the process computer [3]. The simulation accuracy depends on the level of detail of the modeling of the subsystems.

2.3 Experimental setup

This study uses standard tensile specimens like Fig. 1 according to the standard dimensions of the DIN 50125 [10] to ensure workpiece and process quality when process parameters are varied. The energetic comparison and the analysis of the material flows of the two PBF-LB/M machines are carried out with three different standard tensile
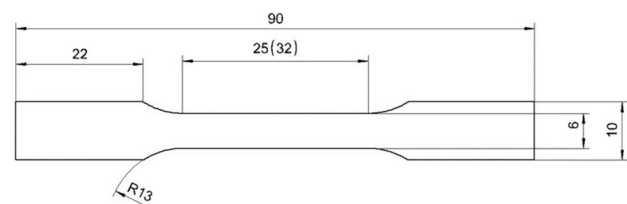
Table 1 Comparison of the additive manufacturing machines used in the test series

	AM400	MPrint
Manufacturer	Renishaw	One Click Metal
Installation space	250 mm × 250 mm × 300 mm	150 mm × 150 mm × 150 mm
Laser power	400 W	200 W
Process	PBF-LB/M	PBF-LB/M
Focus diameter	70 μm	70 μm
Protective gas	Argon	Nitrogen
Vacuum inerting	X	
Materials	316 l, AlSi10Mg, 1.2709	316 l

Fig. 1 Design of a standard tensile test specimen in the Form of type E and a test length of 25 mm

specimens shown in Table 2 manufactured from 316L, a stainless-steel material.

The specimens are manufactured with the standard process parameters of the manufacturer on both machines in different orientations: horizontal, upright and 45°, as it is described by the VDI 3405 [11].

The load curves are recorded with energy data loggers Fluke 1730 and Emonio P3 in the temporal resolution of 1 s. If possible, the different system parts are recorded separately. A higher resolution can be achieved with an oscilloscope, as shown in the study by Brinkmann [12] on the influence of jump times on energy modeling. The oscilloscope allows precise laser power determination at the different scan parameters, strategies, and geometries. Jump times, the phase in which the laser is repositioned until the following point exposure, are largely not considered in previous models but lead to increased simulation accuracy (Table 3).

An exemplary mass study is carried out on both machines with the material 316 l to determine the metal powder flows. Faludi [13] calculates a loss of approx. 18% for the AM250, which is identical to the AM400 except for the laser power. This agrees with other studies, which determine a loss of up to over 20% [4] related to the fused metal powder, especially with the production machines without integrated powder handling. Manual sieving is more tending to make mistakes, so it can be expected that the MPrint's cartridge system will result in less loss. Initially, powder quantities are weighed for filling the cartridges and silos. Both machines are filled to the maximum. After production, all containers are again emptied, sieved, and weighed before restoring the initial state. The complete powder stream's recycling degree is determined in this case, which varies from Faludi and Kellen's approach [4, 13].

Simulation accuracy has to be defined to compare the energy models' accuracy. The ACC is introduced by Yi et al. [9] and calculated as shown in Eq. 2.1 with $E_{\exp}$ as the measured energy consumption and E_{sim} for the simulated energy consumption:

$$\text{ACC} = \left(1 - \frac{\left|E_{\exp} - E_{\text{sim}}\right|}{E_{\exp}}\right) \cdot 100\% \qquad (2.1)$$

3 Main chapter(s)

3.1 Determination of the material flows and process gases

The AM400 is initially filled with 103.7 kg of metal powder. The production process melts 1.2 kg, and after unpacking, sieving, and refilling, losses of 1.8 kg are determined. Due to the small sample quantity at MPrint, two build jobs with standard tensile samples were weighed together. With a total powder quantity of 39.6 kg, the value of the waste powder is 398 g, corresponding to a value of around 1% of the total amount sieved. The recycling rates of the AM400, with 97%, are comparable to the MPrint, with 98%, despite manual powder handling. The comparison of all measured weights is shown in Table 4. The waste powder rates related to the components are up to 150%, significantly higher than the values of Faludi and Kellens [4, 13].

Table 5 compares two the principles and built time of tensile specimens. In the AM400, after the vacuum process, inert gas is pulsed in only to maintain pressure and atmosphere. Vacuuming is efficient concerning the required inert gas but requires additional electrical energy.

Table 2 Standard tensile test samples. A testing of round samples is recommended by the VDI 3405 [11] and is used additionally to the already used flat specimen

Tensile test specimen (DIN 50125)	Form	Test length (mm)
E2x6x25L90	Flat	25
E3.25x6x50L98	Flat	50
A5x25	Round	25

Table 3 Measurement of resource flows

Resource	Measuring method	Unit	Uncertainty
Electrical energy	Load study	1 s	<1%
Compressed air	–	m³/h	10–20%
Metal powder	Mass study	g	AM400 (± 100 g) MPrint (± 0.1 g)
Inert gas (argon, nitrogen)	Reading of the cylinder pressure (manometer)	m³	10–20%
Consumables	–	Quantity	–

Table 4 Comparison of the metal powder and waste powder of the AM400 and the MPrint. The recycling rate relates to the whole infilled powder mass

	AM400	Mprint
Infill powder mass	103.7 kg	39.59 kg
Parts mass (with support)	1.2 kg	0.31 kg
Waste powder	1.8 kg	0.398 g
Recycled powder mass	100.7 kg	38.9 kg
Recycling rate	97.1%	98.3%

Table 5 Comparison of the build time and process gas values

	AM400	MPrint
Build time	30 h	12 h (two jobs)
Gas	Argon	Nitrogen
Volume	0.50–0.75 m^3	2.75 m^3

3.2 Analysis of the load curves

The load studies were performed with data loggers with a resolution of 1 s. The high resolution shows individual layers' power curve but does not precisely reflect the laser power since the exposure times are well below 1 s. The load curve of the AM400 shows the different phases of the manufacturing process, as in Fig. 2 visible.

After the start-up of all systems, the base load is approximately constant at 350 W. The inertization process starts at minute 6 when the vacuum pump shows a significant power curve. The deflection at minute 15 is another short activation of the vacuum pump, minutes 16 and 18, and the constant load beginning in minute 19 results from the process gas fan. From minute 30, the melting process starts. The individual layers are recognizable due to the volatile high power above 1000 W, generated by the pulsing laser, as well as the drop in power during the coating process. The layer time, starting with the support structures, is 90 s, and the recoater time is 8.5 s (Fig. 3).

The dryer and cooling unit are external devices and are recorded separately. Figure 3 shows two complete, identical build jobs, each with the AM400 and the cooling and drying unit measured. The power of the cooling and drying unit can be reported as approximately constant at 1900 W. In build job 2, the build platform heating was additionally activated, which heats the build space to 150 °C. In addition to the higher energy requirement, the processing time is extended due to the heating and cooling phases.

The MPrint does not require an external cooling unit. The load curve, shown in Fig. 4, can also be divided into different phases, although less clearly compared to Fig. 2.

The base load is approx. 160 W. From minute two, flooding with nitrogen starts with a slightly increased power of 300 W–350 W. The melting process starts from minute 8:30. The layers are also clearly visible here with a maximum capacity of up to 1200 W. In the comparison of both production machines, the maximum power in the production process is up to 1200 W. The manufacturing parameters are similar due to the same tensile specimens and material. The

Fig. 2 Analysis of the load curve of the AM400. The different phases of the manufacturing process are visible
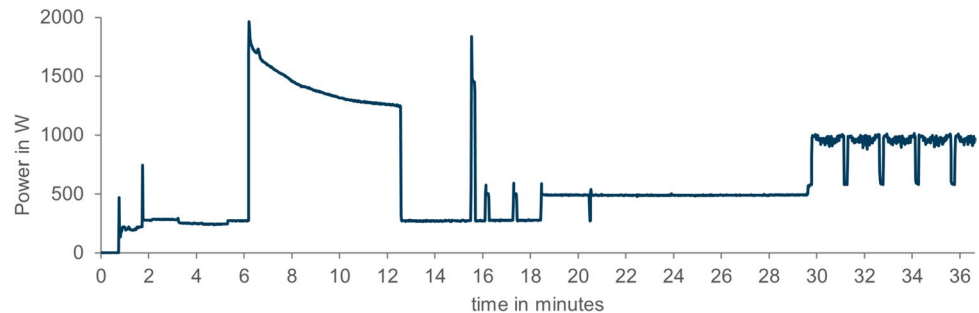
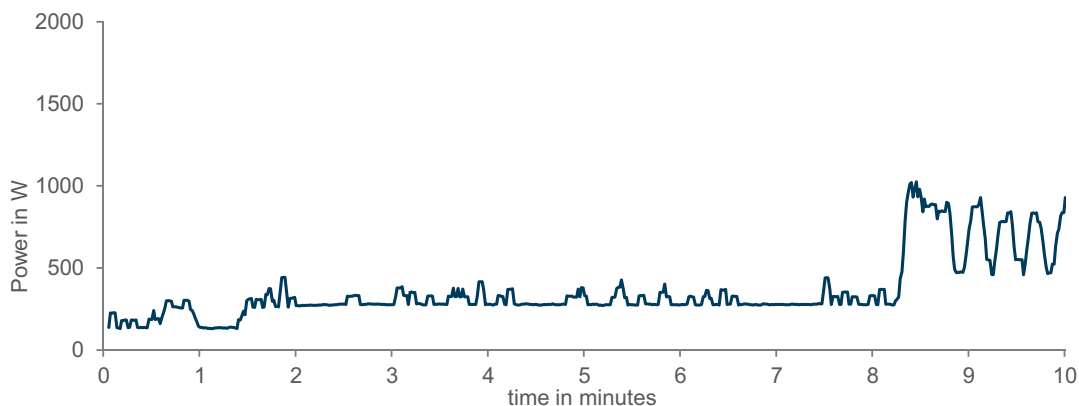**Fig. 3** Comparison of the load curve of the AM400 with and without heating the build plate
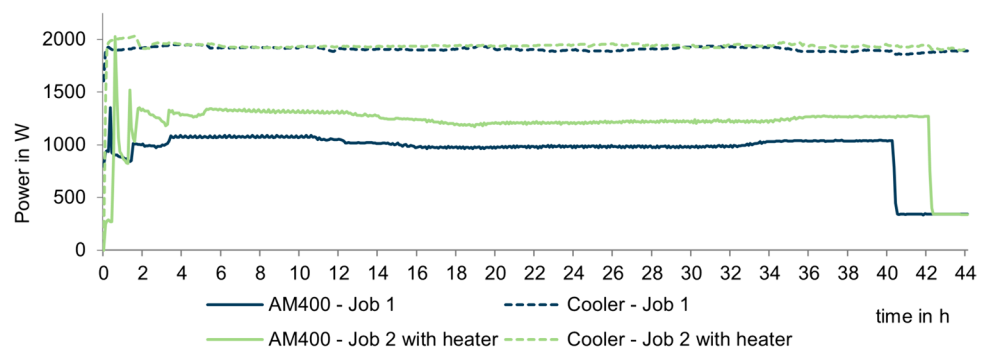
Fig. 4 Analysis of the load curve of the MPrint

base load of the AM400 is higher than that of the MPrint, which does not require an external cooling unit. If this is included with the AM400, the production process's power rises to 3500 W. The slightly longer vacuuming and flooding process of the AM400 saves inert gas by a factor of four, although the volume to be inerted is six times higher.

3.3 Energy consumption

The energy consumption of both additive manufacturing machines is comparable, although the consumption of the AM400 is higher in all sub-phases, as shown in Fig. 5. Without considering the cooling unit, the consumption of 9.4 kWh of the AM400 is higher than that of the Mprint, with 7.4 kWh building the same built job. One reason is the bigger size of the AM400, which also leads to bigger process fans, drivers, and a higher-powered computer and laser system.

3.4 Energy model

The analysis of the load curve helps to understand and optimize an energy model. In contrast to static models, such as the SEC model, this energy model is more based on the analysis of the system and power curves. The model can be described more like the sub-system models but also has characteristics of the sub-phase models due to its division into phases like it is shown in Fig. 6:

$$t_{\text{total}} = t_{\text{Uprep}} + t_{\text{vac}} + t_{\text{Mprep}} + t_{\text{built}} \qquad (3.1)$$

The preparation phase is further subdivided into operator preparation phase t_{Uprep}, vacuum phase t_{vac}, and machine preparation phase t_{Mprep}. Together with the build phase, this results in the total printing duration t_{total} as defined by Eq. 3.1.

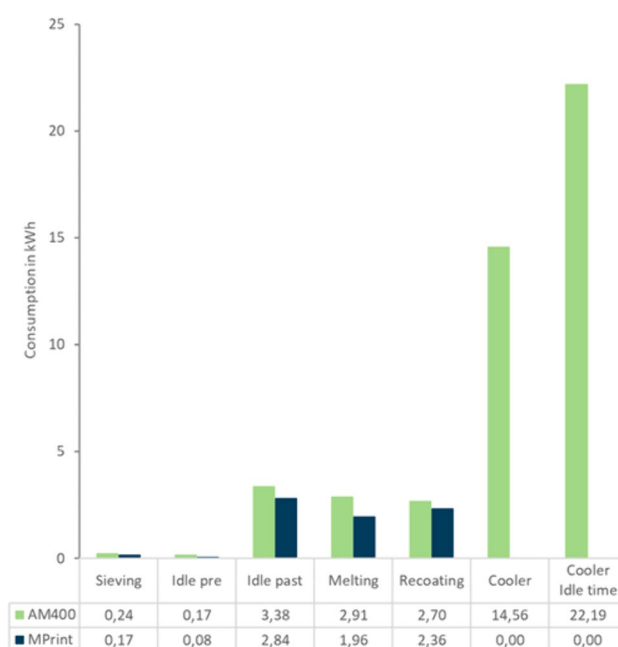|	Sieving	Idle pre	Idle past	Melting	Recoating	Cooler	Cooler Idle time
AM400	0,24	0,17	3,38	2,91	2,70	14,56	22,19
MPrint	0,17	0,08	2,84	1,96	2,36	0,00	0,00

Fig. 5 Comparison of the energy consumption of the AM400 and the Mprint in the sub phases. Obviously, the consumption of the cooling unit is higher than the production process itself

The AM400's cooling and drying unit is considered as a sub-system, depending on the build time. Power functions are developed for the sub-phases, as in the detailed modeling of Yi et al. [9]. The workpiece geometry and process parameters define the properties of the build phase. Therefor a specific time model is necessary with the results from the times of one layer. A special feature is the consideration of jump times [12], which can further increase the accuracy of the energy model. The jump times depend on the scan strategy and the geometry itself. In this case, the energy model is more accurate due to the detailed time models and the consideration of the parts geometry. The innovation of this
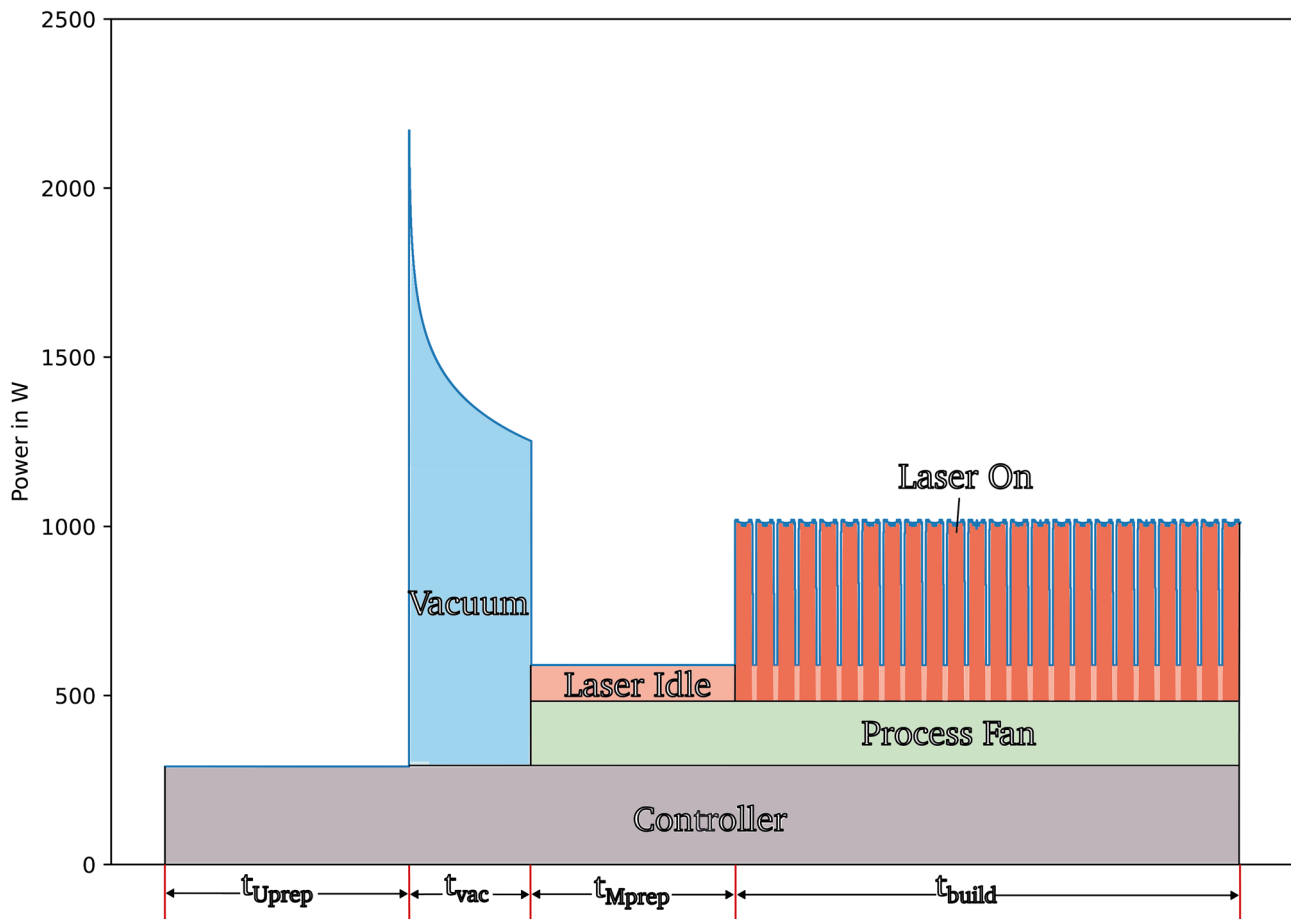
Fig. 6 Example of the sub phase and sub system energy model of the AM400

Table 6 Comparison of the ACC of different energy models

Model	Sample size	ACC$_E$ (average) (%)
Yi et al. [9]	1	98.5
Lv et al. [3]	2	89.4
Baumers et al. [5]	3	94.8
SEC Model (AM400)	6	89.4
Excel Model (AM400)	7	89.5
Python energy simulation	7	95.4

model and the higher accuracy is mostly driven by the combination of the consideration of the geometry of the parts using the built file and the detailed separation of the different sub systems and phases.

The quality of the energy model can be classified by comparing it to the other studies. As shown in Table 6, the ACC of the developed energy model is comparable to the other studies. Considering the jump times and the part's geometry, a higher ACC up to 95.4% is reachable, although the values of Yi and Baumers are higher. However, it is necessary to note that Yi's results were validated only through a case study with a single workpiece. The present study's findings indicate that the simulation accuracy of all examined energy models is subject to workpiece-dependent fluctuations, thus limiting the significance of samples with few workpieces.

4 Discussion

In the study of the resource efficiency of AM processes, electrical energy, process gas, and metal powder are the primary resources.

The mass study shows a high degree of recycling for both units and high losses concerning the component weight. It must be differentiated here that the study's objective was the recycling rate, which is why all the metal powder was sieved. With the AM400, the mass study was carried out highly efficiently and without errors, which can only sometimes be guaranteed. Therefore, it can be challenging to transfer these values to the industry. The integrated powder handling of the

Table 7 Specific energy consumption (SEC) for different studies

Study	SEC for 316L in MJ/kg
Kellens et al. [16]	96.8
Baumers et al. [5]	111.6–139.5
Yi et al. [7] (incl. cooler)	341.31
Brinkmann, Dörr (AM400)	83.2–87.0
Brinkmann (OCM)	60.9–117.3

MPrint has a similarly high value of the recycling rate and the process can be transferred easily to an industrial process.

The production of high-purity process gases such as nitrogen and argon are very energy-intensive [14]. Additional vacuuming shows a high savings potential compared to the pure displacement of oxygen, with an energy consumption of the vacuum pump of approximately 0.1 kWh per build job. Further savings potential can be found in the design of the process gas flow and the design of the installation space. Flow-optimized channels reduce the energy consumption of the circulation and the oxygen residual formation. Despite identical installation space, the value of up to 0.75 m^3 of the AM400 observed over several construction jobs is significantly different from Faludi's estimate of 0.208 m^3 [13]. His estimate is based only on the double calculated volume of the build chamber with 0.11 m^3. It does not consider the likewise evacuated volume of the platform chamber with an additional 0.25 m^3. A total of 0.36 m^3 has to be evacuated, and neither process air, filters, hoses, the set value of oxygen content in ppm, nor the displacement are taken into account. Nevertheless, the comparison shows that the usage of a vacuumization reduces the usage of process gases significantly.

The examination of the load curve shows a high dependence of the energy demand on the build time. During recoating and the jumps, no production takes place despite the increased energy demand. Optimizations are possible here, especially in the design and preparation phase. Implementing a design methodology adapted to AM [15] can lead to significant savings.

Upon analyzing the systems, it is noticeable that the cooling unit of AM400 utilizes a consistent 1900 W of power regardless of the build process's power parameters. A controlled alternative or a cooling water system connection offers a high savings potential.

A high level of detail in the time model of the energy simulation leads to improved simulation accuracy compared to pure SEC models and the parameter-based simulation of the partial phases. The comparison of the SEC in Table 7 shows that the MPrint lies with the upper value in the range of the Baumers study [5]. The minimum value of 60.9 MJ/kg is not comparable to other research, although the batch size of two must also be considered here. The values of the AM400, on the other hand, are verified by a sample of seven

build jobs examined and are in the range of the current study by Kellens [16].

5 Conclusion and outlook

The additive manufacturing process is a resource-intensive manufacturing process [17] representing an innovative tool in various manufacturing systems. Compared to conventional manufacturing systems, the extended degrees of freedom can lead to high savings already in the design phase.

Our research shows high potential for the further development and optimization of system components concerning resource requirements such as electricity or inert gases. Considering component geometry, the methodology for accurate simulation of energy consumption offers additional potential that can be realized directly in the design phase. The transformation process towards climate-friendly and sustainable manufacturing of efficient products can be significantly supported by applying a design methodology adapted to additive manufacturing in combination with resource-efficient design. In particular, the metals industry and manufacturing processes are energy-intensive and have high CO2 emissions. Optimizations based on our simulation of resource consumption support the transformation process towards climate-friendly production.

Declarations

References

1. Brinkmann J, Bremer M, Huwer A, Hoffmann L, Wahl M, te Heesen H (2022) Nachhaltigkeit und Digitalisierung, additive Fertigung und innovative Prozesse. In: Leal Filho W (ed) Nachhaltigkeit in den Natur- und Sozialwissenschaften. Peter Lang Verlag, Berlin, pp 309–336. https://doi.org/10.3726/b19330.

2. te Heesen H, Wahl M, Bremer M, Huwer A, Messemer J (2020) Heterogene Einsatzfelder der generativen Fertigung. Ind 4.0 Manag 2020(4):25–29. https://doi.org/10.30844/I40M20-4S25-29

3. Lv J, Peng T, Zhang Y, Wang Y (2021) A novel method to forecast energy consumption of selective laser melting processes. In J Prod Res 59(8):2375–2391. https://doi.org/10.1080/00207543.2020.1733126

4. Kellens K, Yasa E, Renaldi R, Dewulf W, Kruth JP, Duflou JR (2011) Energy and resource efficiency of SLS/SLM processes. In: 22nd Annual international solid freeform fabrication symposium—an additive manufacturing conference, SFF 2011, no. 22

5. Baumers M, Tuck C, Bourell D, Sreenivasan R, Hague R (2011) Sustainability of additive manufacturing: measuring the energy consumption of the laser sintering process. Proc Inst Mech Eng Part B J Eng Manuf 99:99. https://doi.org/10.1177/0954405411406044

6. Paul R, Anand S (2012) Process energy analysis and optimization in selective laser sintering. J Manuf Syst 31(4):429–437

7. Yi L, Krenkel N, Aurich JC (2018) An energy model of machine tools for selective laser melting. Procedia CIRP 78:67–72

8. Hui J, Huang J, Yan Z, Zhang H (2021) Energy Consumption Model for pulse-laser Selective Laser Melting. J Phys Conf Ser 2009(1):012067. https://doi.org/10.1088/1742-6596/2009/1/012067

9. Yi L, Glatt M, Kuo T-YT, Ji A, Ravani B, Aurich JC (2020) A method for energy modeling and simulation implementation of machine tools of selective laser melting. J Clean Prodn, 263:121282. https://doi.org/10.1016/j.jclepro.2020.121282

10. D. 50125 (2016) "DIN 50125—Prüfung metallischer Werkstoffe—Zugproben. Beuth, Berlin

11. VDI 3405 (2013) VDI 3405 Blatt 2—Additive Fertigungsverfahren—Strahlschmelzen metallischer Bauteile—Qualifizierung, Qualitätssicherung und Nachbearbeitung. Verein Deutscher Ingenieure

12. Brinkmann J, Dörr C, te Heesen H (2023) Einfluss von Sprungzeiten in der Energiemodellierung von additiven Fertigungsprozessen mit Metallpulver. RTE J. https://doi.org/10.58134/fh-aachen-rte_2023_005

13. Faludi J, Baumers M, Maskery I, Hague R (2017) Environmental impacts of selective laser melting: do printer, powder, or power dominate? J Ind Ecol 21:144–156. https://doi.org/10.1111/jiec.12528

14. Dopler M, Weiß C (2021) Energy consumption in metal powder production. BHM Berg-Huettenmaenn Monatsh 166:2–8. https://doi.org/10.1007/s00501-020-01068-w

15. Hoffmann LJ, Brinkmann J, Huwer A, Wahl M, te Heesen H (2022) Praxisorientierte Konstruktion in der additiven Fertigung. Zeitschrift für wirtschaftlichen Fabrikbetrieb 117(1–2):30–34. https://doi.org/10.1515/zwf-2022-1013

16. Kellens K, Mertens R, Paraskevas D, Dewulf W, Duflou J (2017) Environmental impact of additive manufacturing processes: Does am contribute to a more sustainable way of part manufacturing? Proc CIRP 61:582–587

17. Brinkmann J, te Heesen H (2021) Ressourcenbedarf von additiv gefertigten Zugproben bei Variation der Orientierung. In: Proceedings of the 17th Rapid.Tech 3D Conference, vol 17, pp 103–114